miR-34a is not a candidate tumor suppressor

Sophie Mockly[1], Élisabeth Houbron[1] and Hervé Seitz[1,2]

1. Institut de Génétique Humaine, UMR 9002 CNRS and university of Montpellier, Montpellier, France

2. Corresponding author; telephone: (+33)434359936; fax: (+33)434359901; email: herve.seitz@igh.cnrs.fr

Keywords: microRNA; miR-34; proliferation; tumor suppressor

The miR-34a microRNA (miRNA) is currently thought to act as a tumor suppressor: its locus is frequently deleted in human tumors and it is believed to repress cell proliferation. We re-visited the evidence of its anti-cancer activity. Our results show that miR-34a is not generally down-regulated in primary tumors relatively to normal adjacent tissues, and the occasional deletion of *miR-34a* in human cancers is not due to an anti-tumorigenic activity of that gene, but rather, to its genomic proximity with an actual tumor suppressor. Its anti-proliferative action was observed upon large, supra-physiological transfection of synthetic miR-34a in cultured cells, and our data indicates that endogenous miR-34a levels do not have such an effect. We thus conclude that the generally accepted tumor-suppressive function of miR-34a is erroneous.

The miR-34 microRNA family comprises six members in human and in mouse: miR-34a, miR-34b, miR-34c, miR-449a, miR-449b and miR-449c (Extended Data Fig. 1). The three miR-34a/b/c subfamily members are transcriptionally controlled by the p53 tumor suppressor, which suggested that these miRNAs could participate in the tumor suppressive activity of the p53 network [1, 2, 3, 4, 5, 6, 7]. Indeed, the miR-34a member is down-regulated or lost in various cancer models (tumor samples or transformed cell lines) relatively to normal samples [1, 3, 8, 2, 6, 9, 10, 11, 12]. Yet its murine ortholog does not display any obvious tumor-suppressing activity [13].

It is now possible to compare miRNA levels between tumors and normal adjacent tissues on a large collection of human cases [14], allowing a rigorous assessment of miR-34 expression in tumorigenesis. Human primary tumors tend to over-express miR-34a (Fig. 1**a**), contradicting the notion that miR-34a silencing could participate to tumorigenesis.

When it occurs, the occasional deletion of the *miR-34a* gene in cancers also appears to be due to confounding causes. *miR-34a* is located on cytogenetic band 1p36, which is often altered in a wide variety of cancers. But, whenever a limited region of consistent deletion could be mapped, that region excludes *miR-34a* (with the only exception of myelodysplastic syndromes, but with low experimental support; [15]): see Fig. 1**b**. In fact, a very convincing tumor suppressor is already known at 1p36: the *CHD5* gene [16]. Chromosomal deletions can be very large, and *CHD5*-containing deletions can also encompass the *miR-34a* gene [1], resulting in an enrichment in *miR-34a* deficiencies – even though the actual driver for deletion selection is probably *CHD5*, whose anti-proliferative action is clearly established. Accordingly, small-range genetic alterations in cancer, which would only affect the miRNA gene (short sequence variation, copy number variation) are very rare for the miR-34 family (Fig. 1**c**, **d**; Extended Data Fig. 2).

Numerous studies, based on cultured cell lines, showed that miR-34 transfection inhibits cell proliferation [8, 1, 3, 4, 5, 6, 7], also suggesting a tumor-suppressive role for the miR-34 family. miRNA over-expression generates false positives, raising the possibility that this reported anti-proliferative role is artifactual [22]. We thus deleted the *miR-34a* gene in HCT-116 cells, where miR-34 has been proposed to be anti-proliferative by several independent studies [1, 3, 6] (mutation strategy in Extended Data Fig. 3). Deletion of the *miR-34a* locus eliminated 94% of the expression of the whole miR-34 family (Fig. 2**a** and **b**). Our results do not show any significant difference in the growth rate of *miR-34a*$^{-/-}$ and wild-type clones (Fig. 2**c**). We also prepared *miR-34a*$^{-}$ clones from the human haploid HAP1 cell line, where miR-34a is also not anti-proliferative (it is even slightly pro-proliferative; Extended Data Fig. 4). We also failed to observe significant differences between wild-type and mutant clones under chemical stress (doxorubicin or 5-fluoro-uracil treatment; Extended Data Fig. 5).

In agreement with published data [1], we did observe a strong reduction in cell proliferation when we transfected HCT-116 cells with 100 nM synthetic miR-34, but that effect was lost

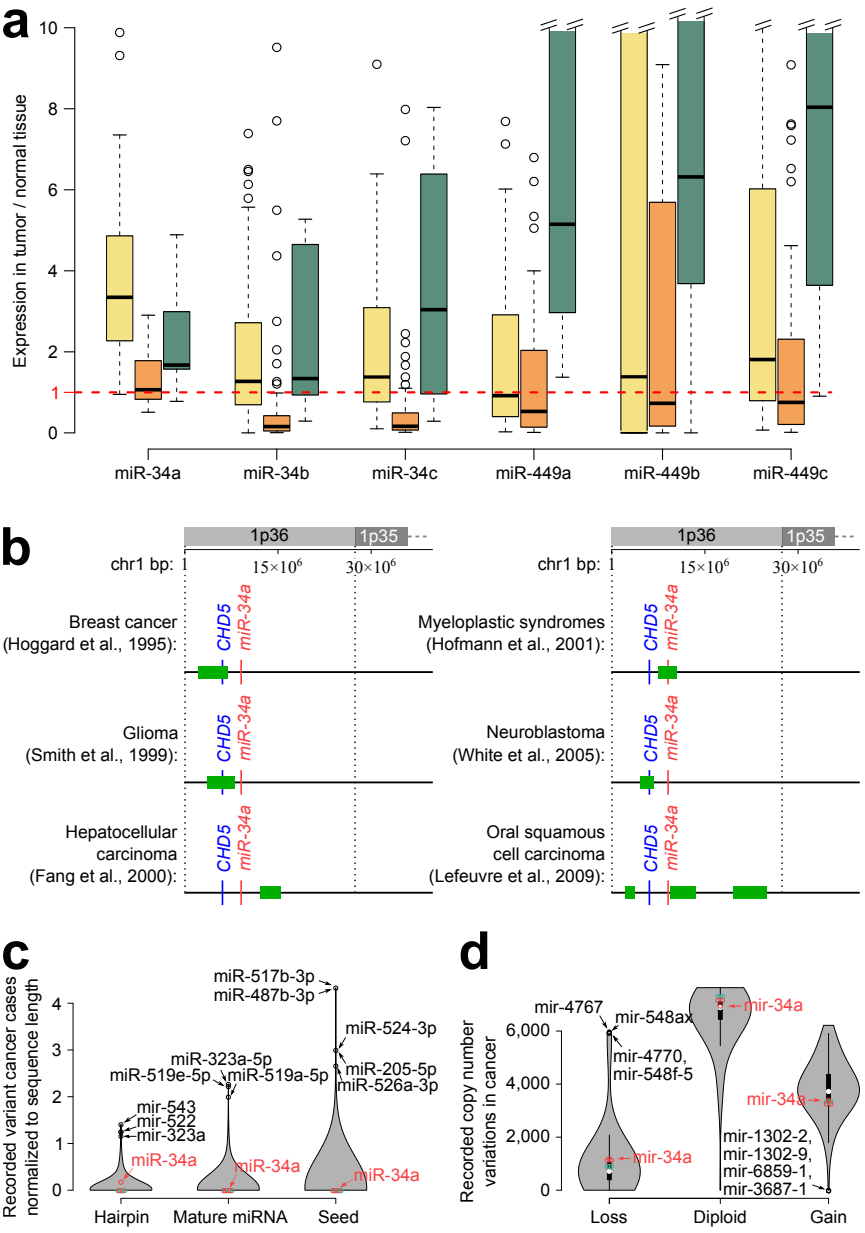

Figure 1: **Human cancers rarely under-express or mutate *mir-34a*. a.** Expression of miR-34 family members in primary tumors relative to adjacent normal tissues (renal carcinoma in yellow, n=69; lung adenocarcinoma in orange, n=70; endometrial carcinoma in green, n=11). The dashed red line indicates a ratio of 1. Ratios larger than 10 are omitted, for graphical clarity. **b.** The 1p36 locus contains 885 annotated coding genes and 36 miRNA genes (Ensembl v.101); for clarity, only *CHD5* (in blue) and *miR-34a* (in red) are shown. Smallest identified region of consistent deletion are in green. Genomic coordinates relate to the hg38 assembly. **c.** Somatic mutations observed in 2,664 human cancers were mapped on miRNA genes. miR-34a/b/c are shown in red, miR-449a/b/c in green. The most frequently mutated miRNAs are shown in black. **d.** Variations in miRNA gene copy number were scored in 11,582 human cancers (NCI Genomic Data Commons). Copy number <2 were flagged as "Loss", >2 were flagged as "Gain". The most frequently lost and the least frequently gained miRNA genes are shown in black. See Extended Data Fig. 2 for miRBase "high-confidence" miRNAs.

when transfecting 10 nM miRNA (Fig. 2**d**). Absolute miRNA quantification by RT-ddPCR shows that a 100 nM transfection over-expresses miR-34a by $> 3 \times 10^4$-fold in HCT-116 cells, clearly demonstrating that such an experiment results in supra-physiological miRNA concentrations (Extended Data Fig. 6).

While the miR-34 family is believed to exert a tumor suppressive action in a diversity of cancers [23], we observed that it is hardly expressed in cultured cell lines, primary tissues and body fluids (Extended Data Fig. 7–9). Current RNA detection technologies can be extremely sensitive, and they can detect miRNAs which are too poorly abundant to induce any clear change in target expression [24]. Hence we anticipate that in all the cell lines for which we analyzed miRNA abundance, and in most cells in the analyzed tissues, miR-34 family miRNAs are actually non-functional.

Yet we do not question the overall functionality of miR-34 miRNAs *in vivo*. Because that family is deeply conserved in evolution (shared between, *e.g.*, vertebrates and insects), it certainly plays important biological functions, perhaps only in a small number of cells, or at very specific developmental stages, where its abundance would be high enough. In mouse, the miR-34 family is particularly expressed in lungs and testes [13, 25]. Mutation of all 6 members of the miR-34 family causes severe ciliogenesis defects, leading to respiratory distress and impaired gametogenesis – translating into sterility and premature mortality [25]. Unsurprisingly then, the most obvious biological functions of that miRNA family seem to take place in the tissues where miR-34 miRNAs are highly expressed, in contrast with the widely-accepted notion of their broad anti-tumorigenic activity.

Acknowledgements

We thank G. Canal, C. Theillet, P.D. Zamore and members of the Seitz lab for critical reading of the manuscript. This research was supported by Cancéropôle GSO "Émergence" grant and Projet Fondation ARC #PJA 20191209613. We thank the MGX facility (Biocampus Montpellier, CNRS, INSERM, Univ. Montpellier, Montpellier, France) for sequencing the Small RNA-Seq libraries.

Author Contributions

S.M. and É.H. performed experiments; S.M. and H.S. performed computational analyses; S.M. and H.S. wrote the manuscript and prepared figures.

Competing Interests statement

The authors declare no competing interests.

References

[1] He, L. *et al.* A microRNA component of the p53 tumour suppressor network. *Nature* **447**, 1130–1134 (2007).

[2] Bommer, G. T. *et al.* p53-mediated activation of miRNA34 candidate tumor-suppressor genes. *Curr Biol* **17**, 1298–1307 (2007).

[3] Chang, T.-C. *et al.* Transactivation of miR-34a by p53 broadly influences gene expression and promotes apoptosis. *Mol Cell* **26**, 745–752 (2007).

[4] Corney, D. C., Flesken-Nikitin, A., Godwin, A. K., Wang, W. & Nikitin, A. Y. MicroRNA-34b and MicroRNA-34c are targets of p53 and cooperate in control of cell proliferation and adhesion-independent growth. *Cancer Res* **67**, 8433–8438 (2007).

[5] Tarasov, V. *et al.* Differential regulation of microRNAs by p53 revealed by massively parallel sequencing: miR-34a is a p53 target that induces apoptosis and G1-arrest. *Cell Cycle* **6**, 1586–1593 (2007).

[6] Tazawa, H., Tsuchiya, N., Izumiya, M. & Nakagama, H. Tumor-suppressive miR-34a induces senescence-like growth arrest through modulation of the E2F pathway in human colon cancer cells. *Proc Natl Acad Sci USA* **104**, 15472–15477 (2007).

[7] Raver-Shapira, N. *et al.* Transcriptional activation of miR-34a contributes to p53-mediated apoptosis. *Mol Cell* **26**, 731–743 (2007).

[8] Welch, C., Chen, Y. & Stallings, R. L. MicroRNA-34a functions as a potential tumor suppressor by inducing apoptosis in neuroblastoma cells. *Oncogene* **26**, 5017–5022 (2007).

[9] Lodygin, D. *et al.* Inactivation of miR-34a by aberrant CpG methylation in multiple types of cancer. *Cell Cycle* **7**, 2591–2600 (2008).

[10] Gallardo, E. *et al.* miR-34a as a prognostic marker of relapse in surgically resected non-small-cell lung cancer. *Carcinogenesis* **30**, 1903–1909 (2009).

[11] Wiggins, J. F. *et al.* Development of a lung cancer therapeutic based on the tumor suppressor microRNA-34. *Cancer Res* **70**, 5923–5930 (2010).

[12] Corney, D. C. *et al.* Frequent downregulation of miR-34 family in human ovarian cancers. *Clin Cancer Res* **16**, 1119–1128 (2010).

[13] Concepcion, C. P. *et al.* Intact p53-dependent responses in miR-34-deficient mice. *PLoS Genet* **8**, e1002797 (2012).

[14] Grossman, R. L. *et al.* Toward a shared vision for cancer genomic data. *N Engl J Med* **375**, 1109–1112 (2016).

[15] Hofmann, W. K. *et al.* Frequent loss of heterozygosity in the region of D1S450 at 1p36.2 in myelodysplastic syndromes. *Leuk Res* **25**, 855–858 (2001).

[16] Bagchi, A. *et al.* *CHD5* is a tumor suppressor at human *1p36*. *Cell* **128**, 459–475 (2007).

[17] Hoggard, N., Brintnell, B., Howell, A., Weissenbach, J. & Varley, J. Allelic imbalance on chromosome 1 in human breast cancer. II. Microsatellite repeat analysis. *Genes Chromosomes Cancer* **12**, 24–31 (1995).

[18] Smith, J. S. *et al.* Localization of common deletion regions on 1p and 19q in human gliomas and their association with histological subtype. *Oncogene* **18**, 4144–4152 (1999).

[19] Fang, W., Piao, Z., Simon, D., Sheu, J. C. & Huang, S. Mapping of a minimal deleted region in human hepatocellular carcinoma to 1p36.13-p36.23 and mutational analysis of the *RIZ* (*PRDM2*) gene localized to the region. *Genes Chromosomes Cancer* **28**, 269–275 (2000).

[20] White, P. S. *et al.* Definition and characterization of a region of 1p36.3 consistently deleted in neuroblastoma. *Oncogene* **24**, 2684–2694 (2005).

[21] Lefeuvre, M. *et al.* Fine deletion analysis of 1p36 chromosomal region in oral squamous cell carcinomas. *J Oral Pathol Med* **38**, 94–98 (2009).

[22] Mockly, S. & Seitz, H. Inconsistencies and limitations of current microRNA target identification methods. *Methods Mol Biol* **1970**, 291–314 (2019).

[23] Slack, F. J. & Chinnaiyan, A. M. The role of non-coding RNAs in oncology. *Cell* **179**, 1033–1055 (2019).

[24] Mullokandov, G. *et al.* High-throughput assessment of microRNA activity and function using microRNA sensor and decoy libraries. *Nat Methods* **9**, 840–846 (2012).

[25] Song, R. *et al.* miR-34/449 miRNAs are required for motile ciliogenesis by repressing cp110. *Nature* **510**, 115–120 (2014).

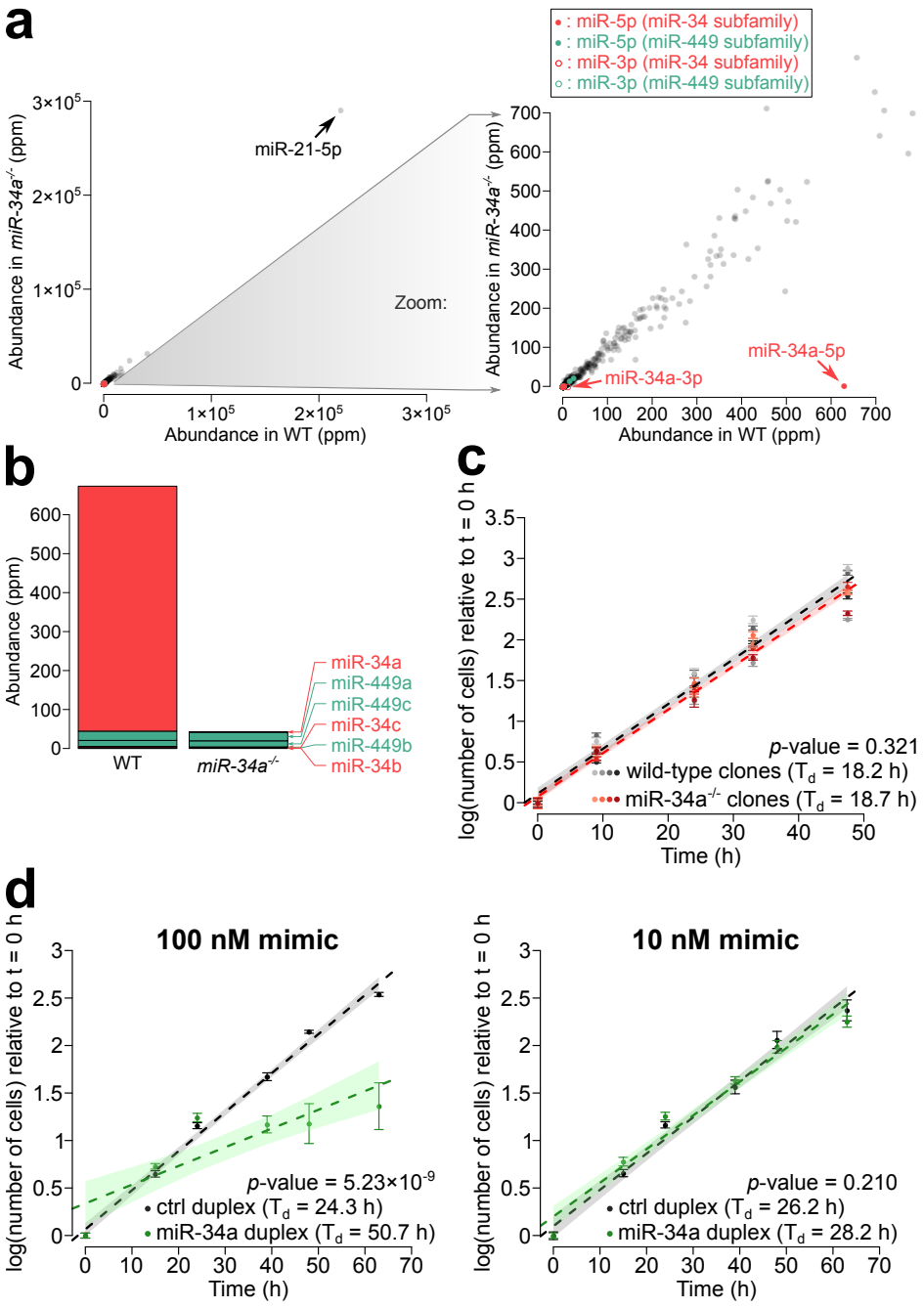

Figure 2: **miR-34 is not a general repressor of cell proliferation. a.** miRNA quantification by Small RNA-Seq in a representative wild-type HCT-116 clone (x axis) and a representative *miR-34a*$^{-/-}$ clone (y axis). Right panel: magnification of the left panel. **b.** Cumulated abundance of miR-34 family members in the two clones. miRNAs are sorted vertically according to their abundance in the wild-type clone. **c.** Four wild-type and four *miR-34a* mutant clones were grown in sub-confluent conditions. Means and standard errors of 4 biological replicates are represented by dots and error bars. **d.** Wild-type HCT-116 cells were transfected with 100 nM (left panel) or 10 nM (right) duplex (either a control siRNA duplex, or miR-34a/miR-34a* duplex) and grown in sub-confluent conditions. Means and standard errors of 6 biological replicates are represented by dots and error bars. **c–d** Linear modeling of log-transformed cell counts relative to time was used to measure doubling time (T_d), and to estimate the significance of the effect of duplex identity (p-values are given in the inset). Shaded areas represent the 95% confidence interval for theoretical future measurements.

miR-34a is not a candidate tumor suppressor

Sophie Mockly, Élisabeth Houbron and Hervé Seitz

Methods

Data and script availability

Deep-sequencing data has been deposited at SRA and linked to BioProject number PRJNA695193. Scripts, raw, intermediate and final data files are available at `https://github.com/HKeyHKey/Mockly_et_al_2021` and at `https://www.igh.cnrs.fr/en/research/departments/genetics-development/systemic-impact-of-small-regulatory-rnas/165-computer-programs`.

Analysis of *miR-34a* mutation in human cancers

Data was downloaded from the GDC portal on October 8, 2020. Matched (tumor and normal tissue) Small RNA-Seq data was available for 938 cases. Focusing on datasets where a primary tumor was matched to a normal adjacent tissue, 69 renal carcinoma cases (for Fig. 1**a**), 70 lung adenocarcinoma cases and 11 endometrial carcinoma cases (for Extended Data Fig. 5) could be extracted. Information about the adjacency of normal tissue controls is from the published literature [26, 27, 28].

GDC cancer mutation data was compared to miRNA genomic coordinates in miRBase v22.1 to extract statistics on the number of mutations per miRNA gene (either in the miRBase-annotated "hairpin" precursor, or in the miRBase-annotated mature miRNA, or in its seed; for Fig. 1**c** and Extended Data Fig. 2), and on the number of miRNA gene losses and gains in human cancers (for Fig. 1**d** and Extended Data Fig. 3).

CRISPR/Cas9-mediated mutagenesis

Four sgRNAs were designed using CRISPOR (`http://crispor.tefor.net/` [29]) to target each side of the human pre-mir-34a sequence, and cloned into an expression plasmid for *S. pyogenes* Cas9 (pSpCas9(BB)-2A-GFP plasmid (PX458), a gift from Feng Zhang [30]; Addgene plasmid #48138; `http://n2t.net/addgene:48138`; RRID:Addgene_48138). Targeting efficiency of each plasmid was estimated by Sanger sequencing of the targeted locus in transfected HCT-116 cells, and analyzed with the Synthego ICE Analysis online tool (`https://ice.synthego.com/#/`). Mutagenesis was performed using the most efficient sgRNA sequence on each side of the targeted locus (AAGCTCTTCTGCGCCACGGT**GGG** and GCCGGTCCACGGCATCCGGA**GGG**; PAM sequences in bold; also see Extended Data Fig. 4).

HCT-116 (ATCC® cat. #CCL-247) and HAP1 (Horizon Discovery cat. #C631) cells were grown till 80% confluency and transfected with the two plasmids (15 µg each) following the protocol for Lipofectamine 2000 Transfection Reagent (Thermo Fisher Scientific). After 24 hours, Cas9-GFP-expressing single cells were isolated in 96-well plates by flow cytometry on a BD FACSMelody (Becton Dickinson), then grown for 10 days. Homozygous wild-type and mutant clones were first tested by discriminative PCRs (with primer pairs ACTTCTAGGGCAGTATACTTGCT and GCTGTGAGTGTTTCTTTGGC; and TCCTCCCCACATTTCCTTCT and

GCAAACTTCTCCCAGCCAAA), and eventually validated by Sanger sequencing of their *miR-34a* locus. For the HAP1 cell line, mutagenesis efficiency was so high that we were unable to isolate wild-type clones after cotransfection of sgRNA-carrying PX458 plasmids. Wild-type clones were therefore generated by transfection of HAP1 cells with a plasmid expressing SpCas9-HF1 variant but no sgRNA (the VP12 plasmid, a gift from Keith Joung [31]; Addgene plasmid #72247 ; `http://n2t.net/addgene:72247`; RRID:Addgene_72247), and went through the same isolation and selection process as mutant clones.

Small RNA-Seq

Cells were plated in 10 cm Petri dishes and allowed to grow for 48 h, then lysed and scrapped in 6 mL ice-cold TRIzol™ Reagent (Invitrogen) added directly to the culture dish after removal of the growth media, and mixed with 1.2 mL of water-saturated chloroform. Samples were homogenized by vigorous shaking for 1 min and centrifuged for 5 min at 12,000 g and 4°C to allow phase separation. The aqueous phase was transfered in a new tube and mixed with 3 mL isopropanol for precipitation. After a 10 min incubation at room temperature, samples were centrifuged for 10 min at 12,000 g and 4°C and the supernatant was removed. The RNA pellet was washed with 6 mL of 70% ethanol and samples were centrifuged for 5 min at 12,000 g and 4°C. After complete removal of ethanol, the RNA pellet was resuspended in 20 µL RNase-free water, the quantity of total RNA was determined by spectrophotometry (NanoDrop ND-1000) and quality was assessed on electrophoretic spectra from a Fragment Analyzer (Agilent), analyzed with the PROSize software (v. 3.0.1.6). Libraries were prepared using NEXTflex™ Small RNA-Seq Kit v3 (Bioo Scientific) following the manufacturer's instructions. Libraries were verified by DNA quantification using Fragment Analyzer (kit High Sensitivity NGS), and by qPCR (ROCHE Light Cycler 480). Libraries were sequenced on Illumina NovaSeq 6000 using NovaSeq Reagent Kit (100 cycles). RNA quality assessment, library preparation, validation and sequencing were performed by the MGX sequencing facility.

Adapters ended with 4 randomized nucleotides in order to reduce ligation biases. Because of the sequencing design, the adapter sequence (5´ GTTCAGAGTTCTACAGTCCGACGATCNNNN 3´) appears at the beginning of the read sequence, and the final 4 nucleotides of the read are the initial randomized nucleotides of the other adapter, whose other nucleotides are not read. Hence small RNA reads can be extracted from the fastq files with the following command:

```
cutadapt -g GTTCAGAGTTCTACAGTCCGACGATCNNNN --discard-untrimmed -m 18 -M 30\
$input_file.fastq | cutadapt -u -4 -
```

Proliferation assays

Because the mere procedure of isolating and selecting mutated clones may artifactually select clones with exceptionally high proliferation rates, we applied the same isolation and selection procedure to wild-type clones, and we measured proliferation rates on several independent wild-type and mutant clones. Each cell line was seeded in 96-well plates (Figure 2**c**: in 4 replicates at 3×10^3 cells/well per time point; Figure 2**d**: in 6 replicates at 1.5×10^3 cells/well). For Figure 2**d**, cells were transfected 24 hours later (either with a control duplex, siRNA against eGFP: 5´-GGCAAGCUGACCCUGAAGUdTdT-3´ / 5´-ACUUCAGGGUCAGCUUGCCdTdT-3´; or with a hsa-miR-34a mimic duplex: 5´-P-UGGCAGUGUCUUAGCUGGUUGUU-3´ / 5´-P-CAAUCAGCAAGUAUACUGCCCUA-3´) according to the protocol for Lipofectamine 2000 Transfection Reagent (Thermo Fisher Scientific).

From 24 hours after cell seeding or transfection, to 3 days later, the number of living cells was determined twice a day by CellTiter-Glo Luminescent Cell Viability Assay (Promega) according to the manufacturer's protocol and recorded with a TriStar LB 941 (Berthold Technologies). Linear regression of log-transformed cell counts relative to time and genotype (in **R** syntax: `log-transformed cell counts ~ time * genotype`) or transfected duplex identity (`log-transformed cell counts ~ time * duplex identity`) was used to measure doubling time and to estimate the significance of the effect of genotype or transfected duplex.

For Extended Data Fig. 6, doxorubicin (Sigma-Aldrich) was diluted in molecular biology-grade water and 5-fluorouracil (5-FU) (Sigma-Aldrich) diluted in dimethyl sulfoxide (Sigma-Aldrich). In a preliminary experiment, half-maximal inhibitory concentration (IC50) was estimated after 72 h drug exposure: 7×10^{-8} M and 8×10^{-6} M for doxorubicin and 5-FU respectively. Cell lines were seeded in 3 replicates per drug concentration at 2.5×10^3 cells/well in 96-well plates. After 24 hours, culture medium was replaced with drug-containing medium (concentration range centered on the IC50 with 2.5× increments), or solvant-containing medium for untreated controls, and the number of living cells was determined 72 h later by CellTiter-Glo Luminescent Cell Viability Assay (Promega). Cell counts were normalized to the mean cell number in untreated controls. Normalized cell number was fitted to an asymptotic model for each clone to assess the significance of the effect of genotype (using an analysis of variance to compare a model not informed by clone genotype, to a genotype-informed model).

miRNA quantification by RT-ddPCR

Reverse transcription of a specific miRNA in HCT-116 cells was performed on 10 ng total RNA using the TaqMan microRNA Reverse Transcription Kit (Thermo Fisher Scientific) in a total volume of 15 µL, according to the manufacturer's protocol, with miRNA-specific RT primers from the TaqMan MicroRNA Assay Kit (assays IDs for hsa-miR-34a-5p and miR-21b-5p are respectively 000426 and 000397). ddPCR amplification of the cDNA was performed on 1.33 µL of each cDNA combined with 1 µL of miRNA-specific 20X TaqMan MicroRNA Reagent containing probes and primers for amplification from the TaqMan MicroRNA Assay Kit (Thermo Fisher Scientific), 10 µL of 2X ddPCR Supermix for probes (no dUTP) (Bio-Rad), and 7.67 µL of molecular biology-grade water. Droplets were generated, thermal cycled and detected by the QX200 Droplet Digital PCR System (Bio-Rad) according to the ddPCR Supermix protocol and manufacturer's instructions. Data were extracted using QuantaSoft Pro Software (Bio-Rad).

References

[26] Clark, D. J. *et al.* Integrated proteogenomic characterization of clear cell renal cell carcinoma. *Cell* **179**, 964–983 (2019).

[27] Gillette, M. A. *et al.* Proteogenomic characterization reveals therapeutic vulnerabilities in lung adenocarcinoma. *Cell* **182**, 200–225 (2020).

[28] Dou, Y. *et al.* Proteogenomic characterization of endometrial carcinoma. *Cell* **180**, 729–748 (2020).

[29] Concordet, J.-P. & Haeussler, M. CRISPOR: intuitive guide selection for CRISPR/Cas9 genome editing experiments and screens. *Nucleic Acids Res* **46**, W242–W245 (2018).

[30] Ran, F. A. *et al.* Genome engineering using the CRISPR-Cas9 system. *Nat Protoc* **8**, 2281–2308 (2013).

[31] Kleinstiver, B. P. *et al.* High-fidelity CRISPR-Cas9 nucleases with no detectable genome-wide off-target effects. *Nature* **529**, 490–495 (2016).